B7 – 1

A Study of Scatter-to-Primary Dose Ratio in Stereotactic Irradiation

Hiroki Ohtani [1], Toraji Irifune [1], Crister P Ceberg [2], Sven-Erik Strand [2], Hidetoshi Saitoh [1], Masahiro Fukushi [1], Tsuguhisa Katoh [1]

1) Tokyo Metropolitan University of Health Sciences,
2) Lund University Hospital, Sweden

INTRODUCTION

Most dose calculation algorithms in stereotactic irradiation are based on data measured in standardized, symmetric geometry with large field. It is important to tie together large field and small field approaches. The scatter-to-primary dose ratio (SPR) is examined within the framework of the semi-empirical dose-calculation formalism developed by Ceberg et al[1]. Quantities describing the radiation balance in large field, i.e. the SPR and the electron disequilibrium factor, E-factor, were derived from measured large field data[2),3)]. Analytical models of the applicable physical processes were then fitted to the derived data of the SPR and the E-factor, and used to give the smallest field dose.

We discussed the SPR in terms of dosimetry for smallest field at shallow depth for the purpose of evaluating accurate absorbed dose in stereotactic irradiation.

METHOD

The dose kernel may be divided into its primary and scattered components. These parts can be integrated separately to yield the primary, $P(Z,R)$, and the scattered dose, $S(Z,R)$. This gives the SPR:

$$\mathrm{SPR}(Z,R) = S(Z,R) / P_{eq}(Z,R) \qquad (1)$$

The calibration for small square field was performed with 6 MV photon beams from Mitsubishi ML-6M linear accelerator using a MixDP phantom. The measurement was performed using small thimble ionization chamber with nominal ionizing volume of 0.009 ml, known as micro-chamber.

For the determination of SPR$(Z,0)$, relative depth dose curves were measured in a MixDP phantom in the range of square field sizes from 0.4×0.4 cm^2 to 10×10 cm^2. Then data were extrapolated smoothly to zero field size for each depth to exclude the influence of lateral contaminating electrons. We thus obtained the $St(Z,0)$, that is, the combined the dose of primary photon and longitudinal scatter electrons. The $P_{eq}(Z,0)$ was obtained extrapolating values of $St(Z,0)$ to surface of the unit in order to

exclude the influence of all contaminating electrons. The dose of longitudinal scatter electron was calculated by

$$S(Z,0) = St(Z,0) - P_{eq}(Z,0) \quad (2)$$

From these values, SPR(Z,0) was determined by Eq.(1).

For the determination of SPR(0,R), the relative depth dose curves were extrapolated linearly to surface in order to exclude the influence of longitudinal contaminating electrons. We obtained the $St(0,R)$ that is the combined dose of primary photon and lateral scatter electrons. It was assumed the $P_{eq}(0,R)$ was independent of field sizes.

RESULTS

Fig.1 show the tissue maximum ratio (TMR) curves that were drawn for MixDP phantom thickness on each field size. The horizontal axis of this graph represents side of square field and the vertical axis represents the TMR. The gradient of TMR curve on field sizes less than 2×2 cm^2 increases sharply with increase of the phantom thickness in over thickness of 10 cm.

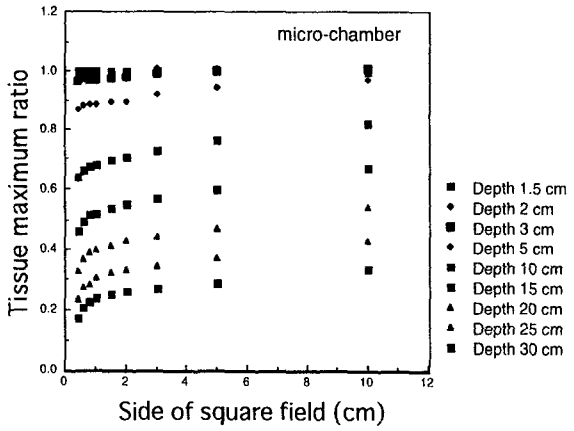

Fig.1 The TMR curves that were drawn for MixDP thickness on each field size.

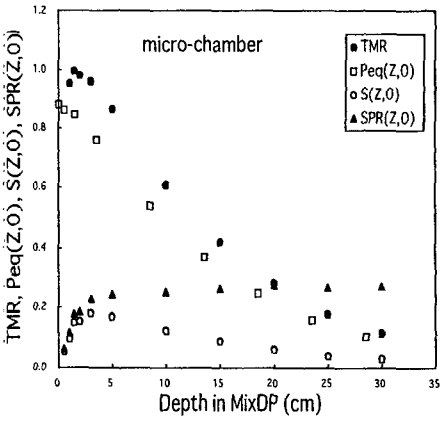

Fig.2 The result that was obtained by extrapolation of the TMR to zero field size, and curves of the Peq(Z,0), the S(Z,0) and the SPR(Z,0).

Fig.2 show the result that was obtained by extrapolation of the TMR to zero field size, which corresponds to the $St(Z,0)$ that is the combined dose of primary photon and lateral scatter electrons for zero field. The extrapolated values for build-up curve consequence were 0.880 by micro-chamber. The $P_{eq}(Z,0)$ showed linear attenuation after the incident of phantom. The difference between the $P_{eq}(Z,0)$ and the $St(Z,0)$ decreases gradually with increase of the depth. Fig.2 show curves of the $S(Z,0)$ and the SPR(Z,0). The $S(Z,0)$ increases to the depth of 3 cm, and decreases with increase of the depth over 3 cm. The SPR(Z,0) increases to the depth of 3 cm, and had a stable value at deep depth. From the results, the share of scatter electron components for primary dose excluded the influence of lateral contaminating electrons was described.

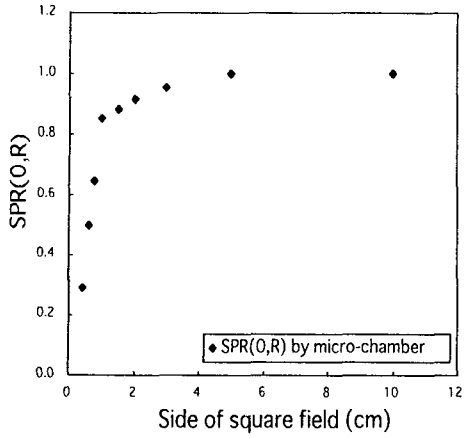

Fig.3 The SPR(0,R) that excluded the influence of longitudinal contaminating electrons.

Fig.3 shows the SPR(0,R) that excluded of longitudinal contaminating electrons. The horizontal axis of graphs represents side of square field. The vertical axis represents the SPR(0,R) that the value on the side of square field of 10 cm was 1.0 which the SPR(0,R) was calculated. The SPR(0,R) curve on field sizes less than 2×2 cm^2 decreases sharply with decrease of the field size, which indicates that the share of scatter electron components decreases with decrease of the field size.

DISCUSSION

From Fig.2 the difference between the $P_{eq}(Z,0)$ and the $St(Z,0)$ decreases gradually with increase of the depth. This is due to a process of attenuation. The primary beams show linear attenuation after the incidence to phantom, but scatter electrons are affected by the energy of primary beams. The contribution of scatter electrons to the dose decreases, because the range of scatter electron is short at the deep depth. From these reasons, it was suggested that $St(Z,0)$ curve was larger than the $P_{eq}(Z,0)$.

The $S(Z,0)$ increases to the depth of 3 cm, and decreases with increase of the depth over 3 cm. The reason of this result is the range of scatter electrons[4),5)]. The contribution of scatter electrons to the dose increases in the area of build-up. However, the dose for scatter electrons decreases at the deep depth, because the energy of scatter electrons decreases with decrease of the energy of primary beams. The SPR(Z,0) increases to the depth of 3 cm, and had a stable value at the deep depth. From this result, it was suggested that the influence of scatter electrons decrease with decrease of the depth. The influence depends on the build-up of high-energy photon beams.

In the lateral components, it was assumed the $P_{eq}(0,R)$ was independent of field sizes. From Fig.3, the share of scatter electron components decreases with decrease of field sizes. This is due to the range of scatter electrons. Lateral components of scatter electrons on small field are not in equilibrium because most scatter electrons fly out from small field. It was useful that the SPR(0,R) was determined by the value of extrapolation to exclude the influence of longitudinal contaminating electrons. The film was reacted by low energy particle because the matter of high atomic number was arranged at lateral direction. This matter was coped by the extrapolation.

This study was performed using small thimble ionization chamber, but this chamber has problems for dosimetry at the shallow depth. Accurate measurement is

affected the relation between field sizes and detector volume. We coped with this problem using the extrapolation technique. However, it is important that measurement is performed using some detectors as shallow chamber or diode detector.

Accurate dosimetry in stereotactic irradiation has some problem, because the lateral components of secondary electrons for smallest field are not in equilibrium. Absorbed dose for smallest field depends on a share of primary beams. The physical characteristics of smallest field at shallow depth were indicated to investigate scatter-to-primary dose ratio. This fact shows that stereotactic irradiation produce an unsteady secondary electron equilibrium.

CONCLUSION

We calculated the SPR(Z,R) using extrapolation technique to exclude the influence of contaminating electrons. The SPR(Z,R) of longitudinal component increases in the area of build-up, and the SPR(Z,R) of lateral component decreases sharply with decrease of field size, which gives a profile of phantom-generated electrons. When the dose evaluation is performed for small field at the shallow depth, the SPR(Z,R) must be considered, and the measurement using some detectors is important. The small thimble ionization chamber used in this study had an advantage that could measure the longitudinal and the lateral components at the same time. We point out importance of the investigation of a relation between primary beams and scatter electrons on theoretical methods or computer simulations.

References

1) Ceberg C P, Bjarngard B E, Zhu T C : Experimental determination of the dose kernel in high-energy x-ray beams. Med Phys 23; 505-511, 1996.
2) Bjarngard B E, Schackford H : Attenuation in high-energy x-ray beams. Med Phys 21; 1069-1073, 1994.
3) Bjarngard B E, Vadash P, Zhu T C : Doses near the surface in high-energy x-ray beams. Med Phys 22; 465-468, 1995.
4) Li X A, Soubra M, Szanto J, et al : Lateral electron equilibrium and electron contamination in measurements of head-scatter factors using miniphantoms and brass caps. Med Phys 22; 1167-1170, 1995.
5) Ohtani H, Irifune T, Saitoh H, et al : Characteristic of radiosurgery x-ray beam with 6 MeV linear accelerator. Bulletin of Tokyo Metropolitan College of Allied Medical Sciences No.8 : 85-90, 1995.